BARRIER-DISCHARGE-PUMPED EXCILAMPS

M.I. Lomaev, V.S. Skakun, E.A. Sosnin, and V.F. Tarasenko

Institute of High-Current Electronics,
Siberian Branch of the Russian Academy of Sciences, Tomsk
Received October 7, 1997

Results of experimental investigations of coaxial and planar barrier-discharge-pumped excilamps are presented. An average radiation power of more than 2 W *has been obtained for efficiency of* 2.6% *with the use of a* XeCl *excilamp. It is shown that the radiation efficiency of the barrier-discharge-pumped excilamps increases with the use of sinusoidal pumping pulses with durations of several tens of microseconds. The excilamps with two emitters pumped by one generator radiating at different wavelengths have been tested.*

INTRODUCTION

Photons with energies 5–10 eV (UV and vacuum UV spectral regions) can initiate and support different chemical, physical, and biological processes (Refs. 1 and 2). Mean- and high-pressure arc discharges in xenon, kripton, and mixtures of mercury with rare gases are traditionally used to generate photons. The radiation spectrum of such sources extends from 200 nm to IR. Meanwhile, the intense radiation in a relatively narrow spectral range is required for a number of processes. In this case the UV-lasers (for example, the exciplex or the nitrogen laser) or comparatively recent excimer and exciplex lamps (excilamps) (Refs. 3–19) can be used.

The use of excilamps in cases in which radiation coherence is not required offers essential advantages. For spontaneous radiation of excimer and exciplex molecules, various types of pulsed, pulsed-periodic, and continuous discharges are used – glow (Refs. 3 and 4), spark (Ref. 5), microwave (Ref. 6), and self-maintained pulsed discharges with UV-preionization (Refs. 7 and 8). In accordance with the review of UV excimer sources of spontaneous radiation (Ref. 9), barrier, UHF-, and discharge-pumped excilamps are most suitable for industrial application.

The barrier discharge (BD) between electrodes to which the high pulsed voltage is applied takes place when a dielectric layer is placed in a discharge gap (sometimes this type of the discharge is named silent discharge). In this case for dense gas media (at a pressure of ~1 atm and more) in the interelectrode gap a specific discharge takes place consisting of many sparks (microchannels or filaments) shaped like pseudocylinders with current densities varying from several ampers to ~1 kA/cm^2. Typical diameters of the cylindrical part of the microchannel are several hundreds of micrometers for discharge durations smaller than 100 ns. The dielectric is used to confine the energy in a single microdischarge and thus the uniform distribution of discharges over the electrode surface is achieved. The average electron energies in individual microdischarges are in the range 1–10 eV and the concentration of electrons is 10^{14}–10^{15} cm^{-3} (Ref. 14). These conditions are similar to those realized in the excimer and exciplex lasers; therefore, the excimer and exciplex molecules derive the energy fed into the medium: collisions between electrons and atoms in the channel lead to excitation and ionization of atoms which at high pressures form excimers and exciplexes before nonradiative deexitation or recombination occurs during "parasitic" processes. The general scheme for obtaining UV and vacuum UV radiation with the use of excimer molecules is the following:

$e + R \rightarrow e + R^{**}$,	excitation	(1)
$e + R \rightarrow e + R^{*}$,	excitation	(2)
$e + R \rightarrow e + R^{+}$,	ionization	(3)
$R^{**} \rightarrow R^{*}(^3P_{1,2})$,	relaxation	(4)
$R^{*} \rightarrow h\nu + R$,	resonant transition	(5)
$R^{*} + R + R \rightarrow R_2^{*}(^{1,3}\Sigma_u^{+}) + R$,	conversion	(6)
$R^{+} + R + R \rightarrow R_2^{+} + R$,	conversion	(7)
$R_2^{*} + e + R \rightarrow R_2^{*}(^{1,3}\Sigma_u^{+}) + R$,	recombination	(8)
$R_2^{*} \rightarrow R + R + h\nu$.	emission	(9)

Finally, according to Eq. (9) the difference between the energies of the bound state $^{1,3}\Sigma_u^{+}$ and the ground repulsive state $^1\Sigma_g^{+}$ is fed in the first and second rare gas emission continuums.

Heteroatomic complexes (exciplexes), for example, monohalides of rare gases RX*, are formed in the following way. In addition to processes described by Eqs. (1)–(9), negative ions of atomic halogen are produced (for example, by dissociation of vibrationally excited molecules of HCl* the negative Cl ions are produced), but the exciplexes are formed through ion-ion recombination and harpoon reactions. The relative contribution of these mechanisms changes as a function of the parameters of the optical medium

0235-6880/98/02–03 243-07 $02.00

$$e + u_2(mu) \rightarrow X^- + X(H), \quad \textit{dissociation} \quad (10)$$

$$R^* + u_2 \rightarrow RX^* + X, \quad \textit{harpoon reaction} \quad (11)$$

$$R^+ + X^- + l \rightarrow RX^* + M. \quad \textit{ion-ion recombination.} \quad (12)$$

The idea of using BD to obtain the rare gas continuum emission was first conceived in Ref. 10, where the hydrogen continuum was excited in the discharge with ceramic electrodes. In 1978 Pavlovskaya et al. (Ref. 10) obtained the continuums in an ozonator (Ref. 11) and perform further investigations of two lamps with radiation output in the direction transverse to the discharge between two extended electrodes bounded by dielectrics (Ref. 12).

Extensive spectral investigation of excimers formed in BD were performed by the group headed by Kogelschatz (Refs. 1 and 13–16). They showed experimentally that BD can be used to obtain narrow-band spectra of the excimer and exciplex molecules using simple methods, which is one of the main advantages of the barrier discharge pumping. Another advantage of the barrier discharge is that the discharge conditions in microgaps – the energy and concentration of electrons – can be optimized adjusting the external parameters such as the discharge gap geometry and types of discharge pumping generator and dielectric. In addition, using the BD in an unsealed tube and placing the electrodes out of this tube, the pure spectrum and the long lifetime of working mixture can be obtained (Ref. 11).

It should be noted that in most papers devoted to BD (Refs. 1, 2, and 13–16) information is lacking about energetics and/or dependences that illustrate the optimum operating conditions of such sources. The argon and kripton continuums of the device with a ceramic electrode and planar BD geometry were also investigated in Ref. 18.

This paper is devoted to the experimental investigation of amplitude-temporal characteristics of radiation of the coaxial and planar barrier-discharge-pumped excilamps.

EXPERIMENTAL SETUP AND MEASUREMENT PROCEDURES

BD is used to develop spherical, planar, and coaxial excilamps. The spherical excilamps still have not been investigated by us. The coaxial excilamp used in our experiments is shown in Fig. 1.

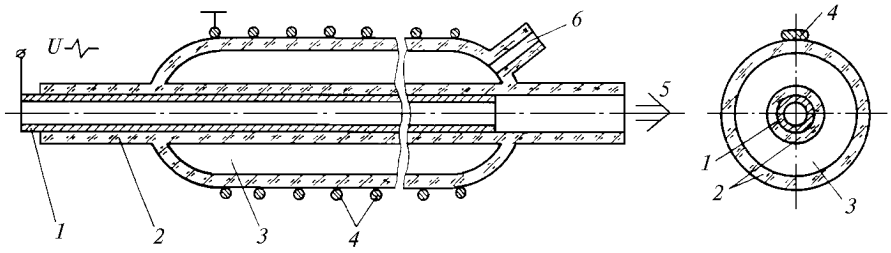

FIG. 1. Design of coaxial barrier-discharge-pumped excilamp: metallic tube (a reflector and a potential electrode) (1), quartz bulb of the lamp (2), gas volume (3), external grid electrode (4), direction of water stream (5), and gas input (6).

The hollow metal potential electrode was placed in the internal tube and the grid electrode with transmission of 82% (or 66%) was placed in the external tube. Two quartz tubes of high quality with transmission of more than 80% in the UV range of spectrum and relatively low transmission at wavelengths less than 260 nm (from 10 to 60%) were used.

In the second case the radiation power of ArF* and KrCl* molecules extracted from the discharge volume was limited by the quartz absorption. For convenience of further presentation, the design parameters of the coaxial excilamps are presented in Table I.

The design of the planar excilamp is shown in Fig. 2. Ceramics with relatively high permittivity from the KVI–3 capacitor, one of the metal plates of which was ground off, was used as a dielectric.

TABLE I. Design parameters of coaxial excilamps.

Excilamp	Number of dielectric barriers	Thickness of discharge gap, mm	Volume of active zone, cm^3	Area of radiating surface, cm^3	Cooling
L1	2	9	193	~ 250	Water
L2	2	7	147	264	Water
L3	2	5	530	~ 1300	Water
L4	1	7	82	164	Natural

The excilamps were excited with four different pulse generators. The first generator (*G*1) (see Fig. 2) consisted of the spark discharger, the K15–10 storage capacitor with a capacitance of 4.7 nF, and the excilamp electrodes connected in series (Ref. 7). This generator was used for pumping both planar and coaxial excilamps.

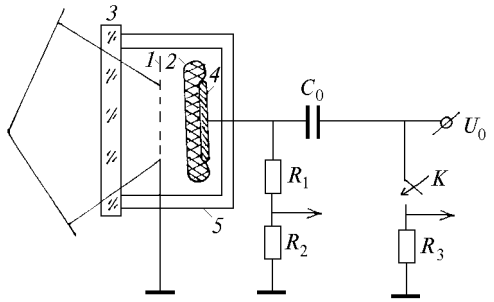

FIG. 2. Design of the planar barrier-discharge-pumped excilamp: grid electrode (1), ceramic electrode with high permittivity (2), quartz window (3), metallic plate (4), and excilamp body (5).

The second generator (*G*2) had analogous circuit schematic, but the TGI–1000/25 thyratron was used as a commutator to trigger the currents up to 10 kA and to operate with pulse repetition frequencies varying from 10 to 4000 Hz at charging voltages 10–28 kV (Fig. 3).

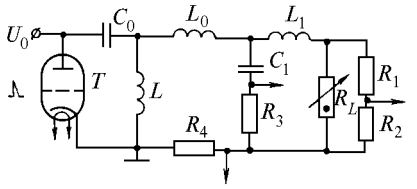

FIG. 3. Circuit schematic of pulse pumping thyratron generator G2: thyratron (T), storage capacitor (0.5–10 nF) C_0, *peaking capacitor* (0.02–6.6 nF) C_1, *charging inductor L, discharge circuit inductor* (~ 30 nH) L_0, *inductor of peaking capacitor discharge circuit* (< 10 nH) L_1, *excilamp* R_L, *resistors of a voltage divider and shunts* $R_1 - R_4$, *input of high voltage* U_0.

In addition the capacitor in this circuit was charged at frequencies higher than 100 Hz from a special generator producing charging pulses with a frequency of ~10 kHz. Therewith after triggering of the thyratron charging of the capacitor C_0 was automatically delayed for about 500 μs.

The third generator (*G*3) was similar to the generator described in Ref. 17. The given circuit schematic (Fig. 4) was used to generate pumping pulses with repetition frequencies varying from 500 Hz to 12 kHz. It produced smaller pumping energy per pulse with alternating polarity. The input section of the generator was the series inventor based on the thyristers D_1 and D_2 with the transformer output Tr_1. When the thyristors were triggered alternatively, the energy from the filter capacitor C_f was transmitted to the capacitor C_1 of the first section of the magnetic generator with alternating polarity of energy pulses. Then the pulse was shortened by the magnetic compression sections on the chokes $L_1 - L_3$ and the coil Tr_1 with a total compression factor of ~100. The step-up transformer Tr_2 with a gain of 2 was placed at the generator output. The generator was connected to the excilamp (*el*) using a 10-meter cable and the balance resistor R_4 = 150 Ω was connected in parallel with the excilamp. The load voltage pulse was bell-shaped with a pulse duration of ~50 ns at half maximum and the voltage pulse amplitude was set in the range 5–16 kV.

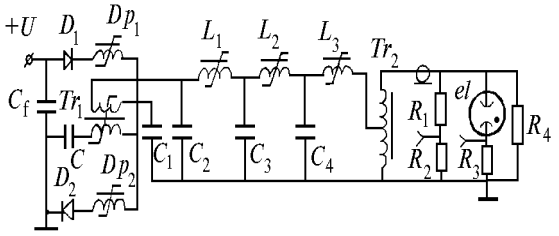

FIG. 4. Circuit schematic of pumping pulse thyristor-magnetic generator G3.

The sinusoidal pulse voltage generator (*G*4) was also used during our experiments. The pulse amplitudes varied from 1 to 10 kV and the pulse durations were several tens of microseconds.

The shunt R_3 and the voltage divider (R_1, R_2) were used for registration of the electric parameters. Amplitude-temporal characteristics of radiation were determined with the use of the FEK–22SPU vacuum photodiode whose output signal was applied at the S8–14 osciloscope. The photodiode input window was bounded by a diaphragm with an area of 1 cm^2. The integral power in the given wavelength range was evaluated using the IMO–2N calorimeter with an input window having an area of 1.5 cm^2.

Optical filters with known transmittance were placed in front of the input window of the IMO–2N to filter out the heat radiation component of the investigated mixtures. Therewith accounting that the time of calorimeter response to the visible and UV radiation is much smaller than the time of heating of the glass from the radiation source, the heat radiation component can be neglected. The integral radiation spectra were registered using the ISP–30 spectroscope on the RF–3 film.

The working mixtures of rare gases and halogens were prepared in the excilamps and in a special mixer during the experiments with the lamp *L*3. Before filling with the working mixture, the gas was evacuated from the lamp and helium or neon were blown through it. Then the lamp was trained with a discharge at a pressure no lower than 1 Torr. Because the length of the lamps significantly increased their cross size, the increase of the radiation power due to the gas mixing was first observed when the lamp was switched on for the first time after the gas mixture preparation.

RESULTS AND THEIR DISCUSSION

The investigated excilamps were filled, as a rule, with the triple mixtures of the working, buffer, and additional gases in the ratios close to those used in the monohalide rare gas lasers. The total pressure of the mixtures during the experiments p_Σ usually did not exceed 1.5 atm ($N < 5 \cdot 10^{19}$ cm^{-3}). The necessary mixture density was achieved by adding of the buffer gases Ar, He, and Ne used to increase the absorbed energy density and to initiate such useful reaction as ion-ion recombination in the presence of the third particle (for example, the formation of KrCl* in the presence of He(Ne) (Ref. 12)). The parameters of radiation in the Ne(He)–Kr–HCl, Ne(He)–Xe–HCl, Ne(He)–Kr–$NF_3(F_2)$, and Ne(He)–Ar–$NF_3(F_2)$ mixtures were investigated. Some obtained results are shown in Figs. 5–13.

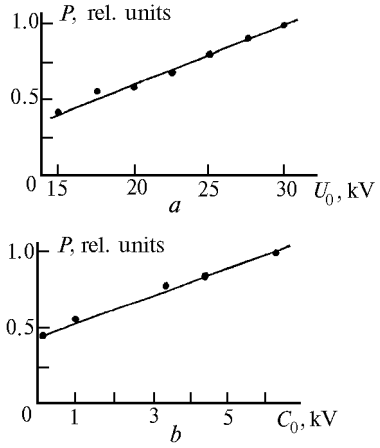

FIG. 5. Dependences of the excilamp pulse power on the storage capacitance C_0 and charging voltage U_0. The total pressure of mixtures was 1 atm. *Lamp L3:* He–Kr–F_2 *mixture,* C_0 = 1.1 nF *(a);* He–Kr–HCl *mixture,* U_0 = 20 kV *(b).*

The dependences of the radiation pulse power of the KrCl and KrF excilamps on the storage capacitance C_0 and charging voltage U_0 are shown in Fig. 5. The increase of C_0 and U_0 leads to the linear increase of the power, but the efficiency of the excilamps does not increase and, as a rule, the maximum efficiency is achieved with small values of C_0 and small discharge voltages. This can be related with the decrease of the energy fed into the plasma relative to the energy stored in the capacitor C_0.

Figures 6 and 7 demonstrate the difference between the operation of the lamp with the single dielectric barrier (*L*4) and two (*L*2) dielectric barriers. The radiation power of the single-barrier lamp decreases for $p >$ (1–1.2) atm (the optimum pressure of the lamp is limited by 0.8–1.2 atm for different gas mixtures), which is caused by the prevalence of individual intense microchannels in the discharge. Meanwhile, the screening of both electrodes by dielectric allows to distribute more uniformly the discharge delivered to the barrier, which provides the uniformity of the energy input at high pressures $p >$ 1 atm (see Fig. 6).

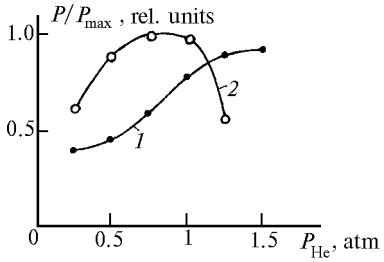

FIG. 6. Dependences between the radiation power in the mixture He:Kr:HCl = P_{He}:45 Torr:3 Torr *and the helium pressure at* U_0 = 30 kV. *Generator G1: lamp L1(1); lamp L4(2).*

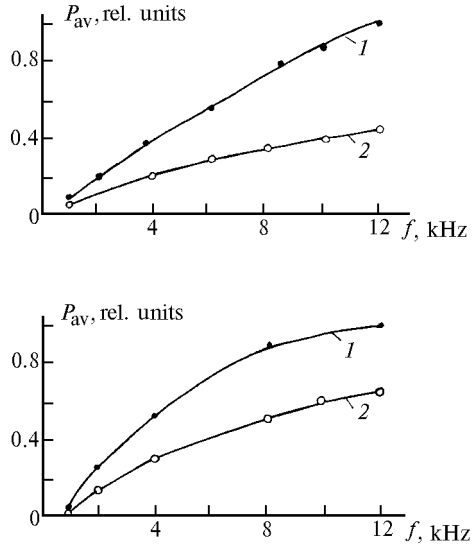

FIG. 7. Dependences between the average power of excilamp radiation and the pumping pulse repetition frequency in lamps L4 (1) and L2 (2) at C_0 = 1.4 nF *and* U_0 = 14 kV *for the mixtures* He:Kr:HCl = 1.25 atm: 45 Torr:3 Torr *(a) and* He:Kr:HCl = 1 atm: 9 Torr:3 Torr.

Almost double power of the excilamp *L*4 with single barrier in comparison with the lamp *L*2 is preserved not only with the increase of the pulse repetition frequency, but also with the change of the buffer gas He on Ne (see Fig. 7). The main disadvantage of the lamp with single barrier under these conditions is the direct contact between the metallic electrode and the discharge, which leads to gradual sputtering of the electrode material and may influence the radiation quality even in the media containing only pure rare gases without additions of such active halogens as Cl and F.

So in Ref. 2 a lifetime of ~40 h was achieved for the single-barrier discharge in the gas mixtures of Xe with argon and neon. Obviously, in the system with

two barriers this time could be significantly increased for the given media.

Figure 7 illustrates the influence of the pumping pulse repetition frequency on the average radiation power. It can be seen that with the increase of the repetition frequency, the average power increases almost linearly. However, for insufficient cooling of the excilamp the given dependence may violate, because more than 60% of the pumping energy per pulse is spent on heating of the excilamp.

Typical waveforms of the voltage pulses on the excilamps, discharge current, and radiation under different conditions of pumping are shown in Figs. 8–10.

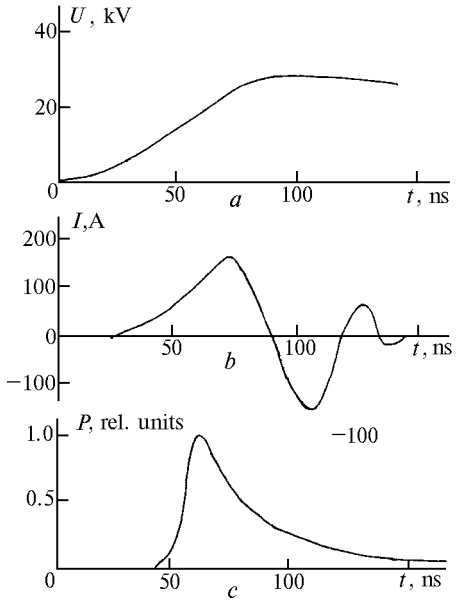

FIG. 8. Waveforms of voltage (a), current (b), and radiation (c) pulses at λ ~ 222 nm *in the excilamp L3 in the mixture* Ne–Xe–HCl *at* C_0 = 1.1 nF and U_0 = 20 kV *with pumping from the generator G2.*

The nanosecond pulse pumping from the generator *G*3 (see Fig. 9) differs from the pumping from the generator *G*2 with smaller pumping pulse energy and, therefore, with smaller energy fed into the active medium. Slow voltage decay on the load (see Fig. 8), typical of the generator *G*2, leads to longer radiation pulse.

The given waveforms were obtained without the peaking capacitor C_1. Its connection may lead to the increase of the spontaneous radiation power, but the pulse energy does not increase. In accordance with the formula for the coaxial capacitor, the capacitance of the excilamp *L*3 filled with plasma cannot exceed ~400 pF. Because the value of the storage capacitance C_0 in most experiments was ≥1 nF, the voltage on the excilamp might exceed the charging one 1.5–2 times (Fig. 8*a*).

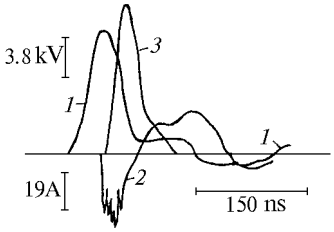

FIG. 9. Waveforms of voltage (1), current (2), and radiation (3) pulses at λ ~ 222 nm *in the excilamp L2 in the gas mixture* He:Kr:HCl = 1 atm:45 Torr:3 Torr *at* C_0 = 1.4 nF *and* U_0 = 14 kV *with pumping from the generator G3.*

In case of the pumping from the nanosecond pulse generators, the typical duration of current pulses did not exceed 200 ns and the radiation pulse duration at half maximum changed from 20 to 300 ns. Long tail (in comparison with that shown in Fig. 9) of the radiation pulse in Fig. 8*c* can be related with slow decay of the voltage pulse from the generator *G*2. It can be expected that the further increase of the voltage pulse duration will lead to the further elongation of the radiation pulse tail, which is confirmed by Fig. 10 illustrating the process of pumping from the nanosecond pulse generator *G*4.

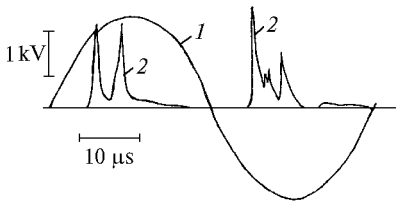

FIG. 10. Waveforms of voltage (1) and radiation (2) pulses at λ = 308 nm *in the excilamp L3 in the gas mixture* Ne–Xe–HCl *at* U_{max} = 2 kV *with pumping from the generator G4.*

It can be seen that in this case the pulse has long tail, which testifies to the prolonged time of energy input in the optical medium. This is also verified by visual observation of the discharge, because the glow patterns after the active medium excitation from the generators *G*1 and *G*3 and from the generator *G*4 are different: in the first case the strimmer phase of the discharge is most pronounced (filaments with clear boundaries, especially well pronounced for p_Σ > 1 atm). In the second case, more uniform glow of the entire volume is observed.

The optimization of mixture for the excilamps *L*2 and *L*3 revealed the following. The increase of the buffer gas pressure first leads to the increase of the radiation intensity and then to the saturation, which for most mixtures does not significantly decrease with the further increase of the pressure up to 1.5–2.0 atm (Figs. 11 and 12). The increase of the halogen pressure leads to the shift of the buffer gas pressure at which the radiation intensity saturates towards smaller pressures.

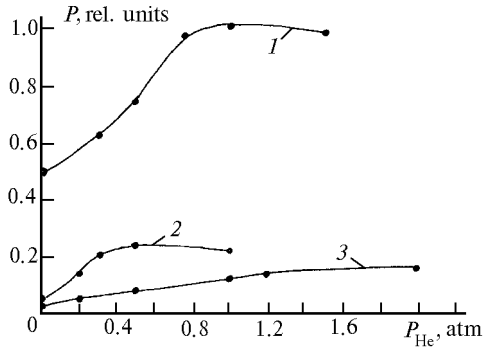

FIG. 11. Dependences between the radiation pulse power and the helium pressure at U_0 = 20 kV *and* C_0 = 1.1 nF *(the generator G2 and the lamp L3) in the gas mixtures* He:Kr:F_2 = P_{He}:100 Torr:5 Torr *(1);* He:Kr:NF_3 = P_{He}:100 Torr:5 Torr *(2);* He:Kr:HCl = = P_{He}:80 Torr:4 Torr *(3).*

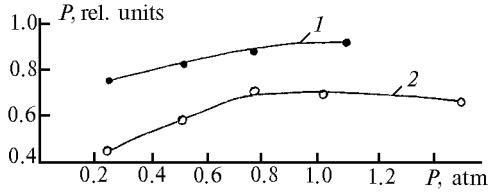

FIG. 12. Dependence between the radiation pulse power in the gas mixtures He*(1)*(Ne*(2)*):Ar:F_2 = = *P*:100 Torr:3 Torr *and the pressure at* U_0 = 20 kV *and* C_0 = 1.1 nF *(the generator G2 and the lamp L3).*

The maximum power of radiation of ArF* molecules for all other factors in all excilamps remaining the same was achieved with He rather than with Ne (see Fig. 11). Meanwhile, in the exciplex XeCl and KrCl lasers with such active media the neon mixtures usually radiate more intense. This can be explained with the fact that in Ne the generation of the electrons and ions is better and the XeCl* and KrCl* molecules in the mixtures with HCl are produced through ion-ion recombination. The ArF* molecules are formed through ion-ion recombination and harpoon reaction as well.

As pointed out in Ref. 13, in most cases the triple reaction by Eq. (12) at typical gas mixture pressures >1 atm is the main reaction for obtaining the exciplex molecules in the barrier discharge, whereas the harpoon channel (Eq. 11) is of secondary importance. The validity of this assumption for the process of exciplex formation under the given experimental conditions can be estimated.

We assume that the main contribution to the formation of exciplexes comes from reactions described by Eqs. (11) and (12). During our experiments on pumping of excilamps from the generators of nanosecond pulses (at total pressures of the mixture ≥1 atm) the concentrations of HCl, F_2, and NF_3 were $4\cdot10^{16} - 3.5\cdot10^{17}$, $9\cdot10^{16} - 2.2\cdot10^{17}$, and $9\cdot10^{16} - 2.2\cdot10^{17}$ cm^{-3} respectively. The rare gas atoms excited through the reaction described by Eqs. (1)–(3) enter the harpoon reaction with halogen molecule described by Eq. (11), if the halogenide density is fairly high

$$V_g[X_2(HX)] > V_{as}N^2 \text{ and } > A, \quad (13)$$

where V_g is the rate constant of harpoon reaction (~10^{-10} cm^3/s for reaction Xe*(Kr*) + HCl and ~ 10^{-9} cm^3/s for reaction Xe*(Kr*) + HF_3); $[X_2(HX)]$ is the concentration of halogen-carrier molecules; V_{as} is the rate of reaction described by Eq. (12); N is the total neutral density (under our conditions at a pressure of 1 atm we use $3.1\cdot10^{18}$ cm^{-3}); and $A \sim 10^5(10^6)$ s^{-1} is the rate of radiative decay of the excited atom of rare gas. From this it follows that during our experiments the concentrations of HCl and HF_3 were deliberately within the limits corresponding to the harpoon reaction.

However, the concentration of the halogen carrier is limited from above

$$V[X_2(HX)] < A, \quad (14)$$

where V is the rate constant of quenching of exciplex with halogenide and A is the rate of radiative decay of exciplex. The criterion (14) is applicable to the experimentally investigated mixtures He–Xe–HCl, He–Kr–HCl, and He–Kr–HF_3. Here, V is equal to $1.4\cdot10^{-9}$, ~10^{-9}, and $52\cdot10^{-12}$ cm^{-3}/s, respectively (Ref. 20), and the rates are $A \sim 2.5\cdot10^7$, ~10^8, and $1.43\cdot10^8$ s^{-1} (Ref. 21). Hence, we obtain that the concentration of halogen carrier does not exceed $1.8\cdot10^{16}$, ~10^{17}, and $2.7\cdot10^{18}$ cm^{-3} in these three cases.

Meanwhile, the experimentally obtained optimum values of [HCl] in the mixtures with hydrogen chloride were 2–5 times larger than this estimation. The increase of the initial concentration of HCl in the volume discharge leads to the decrease of the average electron energy in the discharge and finally to the limited number of exciplex molecules formed through the harpoon reaction (Ref. 19).

Under conditions of the barrier discharge at high pressures when the ion-ion reactions become of primary importance, plasmochemical reactions take place mainly in small volumes occupied with the microdischarges. Therefore, the specific pumping power per unit volume occupied with the discharge filament is significantly higher than in case of the volume discharge. The greatest part of the halogen carrier is out of the pumping region and has no time to enter the microdischarge zones within the time over which the pulse acts. However, as is well known, at high pumping power in the optimum mixture it is necessary to increase the content of the halogen carrier. In this case, limiting condition (14) becomes valid at enhanced concentrations of [HCl] because of quick burn up of the halogen carrier in the microchannel.

The maximum output average power of the coaxial excilamp *L3* with pumping from the generators *G1–G3* was 0.6 and 1.0 W for the KrCl* and KrF* molecules, respectively. The mixtures with F_2 and NF_3, although more energetic (see Fig. 12), had shorter lifetimes. To

the contrary, the use of HCl, which, as our investigations showed, has the better ability to regeneration, provides the maximum time of operation with one portion of the mixture (Fig. 13).

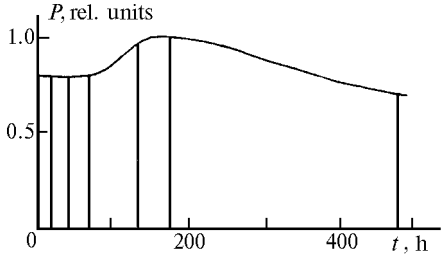

FIG. 13. Dependence between the radiation pulse power at $\lambda \sim 222$ nm *and the lifetime of one portion of the working mixture in the regime of short-time triggering for the gas mixture* He:Kr:HCl = 1 atm:60 Torr:8 Torr at $U_0 = 20$ kV *and* $C_0 = 1.1$ nF *for the number of pulses* $\sim 10^6$.

The increase of the average radiation power was achieved with pumping from the generator *G*4. In this case, as indicated above, the radiation was emitted during the whole time over which the voltage pulse acted (see Fig. 10) including the stages of the short microdischarges and of the volume discharge. So for the gas mixture He–Xe–HCl at $\lambda \sim 308$ mm a radiation power density of 1.7 mW/cm^2 ($f \sim 20$ kHz), an average UV-radiation power of 2.2 W, and efficiency of 2.6% were obtained for the lamp *L*3, whereas with the generator *G*3 ($f \sim 12$ kHz) under the same conditions a power density of ~0.4 mW/cm^2 was obtained for efficiency of ~0.1 %.

It also should be emphasized that the generator *G*2 whose power exceeded several times the power required for one excilamp could be simultaneously connected to two excilamps. It operated on two wavelengths without the decrease of the average radiation power of each excilamp. This allows one to develop excilamps with one pumping generator and two, three, and more emitters operating at different wavelengths.

CONCLUSION

The results of experimental investigations of the coaxial and planar barrier-discharge-pumped excilamps have been presented in this paper. The average radiation power more than 2 W for efficiency of 2.6% has been obtained for the XeCl excilamp. It has been shown that the radiation efficiency of the barrier discharge excilamps increases with the use of sinusoidal pulses with durations of several tens of microseconds. The excilamps with two types of emitters radiating at different wavelength with one pumping generator have been tested.

ACKNOWLEDGMENTS

We are grateful to A.N. Panchenko for his recommendations on measuring of the average radiation power. This paper was supported in part by the Russian Foundation for Basic Researches, Grant No. 96–02–16668a.

REFERENCES

1. H. Esrom and U. Kogelschatz, Thin. Sol. Fil. **218**, 231–246 (1992).

2. F. Kessler and H. Bauer, Appl. Surface Science **54**, 430–434 (1992).

3. A.P. Golovitskii and V.S. Kan, Opt. Spektrosk. **75**, No. 3, 604–609 (1993).

4. A.N. Panchenko, V.S. Skakun, E.A. Sosnin, V.F. Tarasenko, and M.I. Lomaev, Pis'ma Zh. Tekh. Fiz. **21**, No. 20, 77–80 (1995).

5. V.V. Ivanov, V.E. Saenko, and G.V. Rulev, Pis'ma Zh. Tekh. Fiz. **21**, No. 7, 65–68 (1995).

6. H. Kumagai and M. Obara, Appl. Phys. Lett. **55**, No. 15, 1583–1584 (1989).

7. B.A. Koval', V.S. Skakun, V.F. Tarasenko, E.A. Fomin, and E.B. Yankelevitch, Prib. Tekh. Eksp., No. 4, 244–245 (1992).

8. A.A.Kuznetsov, V.S.Skakun, V.F.Tarasenko, and E.A.Fomin, Pis'ma Zh. Tekh. Fiz. **19**, No. 5, 1–5 (1993).

9. M. Obara, in: *Proc. of the 7th Intern. Symp. on the Science & Technology of Light Sources*, (Kyoto, 1995), pp. 149–156.

10. E.N. Pavlovskaya, I.V. Podmoshenskii, and A.V. Yakovleva, Zh. Prikl. Spektrosk. **20**, No. 3, 504–506 (1974).

11. E.N. Pavlovskaya and A.V. Yakovleva, Opt. Spectrosk. **54**, No. 2, 226–231 (1983).

12. G.A. Volkova, N.N. Kirillova, E.N. Pavlovskaya, and A.V. Yakovleva, Zh. Prikl. Spektrosk. **41**, No. 4, 681–695 (1984).

13. U. Kogelschatz, Pure and Appl. Chem. **62**, No. 9, 1667–1674 (1990).

14. U. Kogelschatz, Appl. Surface Science **54**, 410–423 (1992).

15. B. Gellert and U. Kogelschatz, Appl. Phys. **52**, No. 1, 14–21 (1991).

16. U. Kogelschatz and H. Esrom, Laser and Optoelektroniks **22**, 55–59 (1990).

17. N.G. Shubkin, S.P. Sychev, and V.A. Vizir', Prib. Tekh. Ekspr., No. 3, 96 (1990).

18. V.S. Skakun, V.F. Tarasenko, E.A. Fomin, and A.A. Kuznetsov, Zh. Tekh. Fiz. **64**, No. 10, 146–150 (1994).

19. A.M. Boichenko, V.S. Skakun, E.A. Sosnin, V.F. Tarasenko, and S.I. Yakovlenko, Kvant. Elektron. **23**, No. 4, 344–348 (1996).

20. B.M. Smirnov, Usp. Fiz. Nauk **139**, No. 1, 53–89 (1983).

21. M. Obara, *Encyclopedia of Physics, Science and Technology* (Academic Press, Inc.1997), Vol. 7, pp. 190–209.